A Decomposition Algorithm for Simultaneous Scheduling and Control of CSP Systems

Alexander W. Dowling, Tian Zheng, and Victor M. Zavala
Dept. of Chemical and Biological Engineering, University of Wisconsin-Madison, 1415 Engineering Dr, Madison, WI 53706

DOI 10.1002/aic.16101
Published online February 8, 2018 in Wiley Online Library (wileyonlinelibrary.com)

We present a decomposition algorithm to perform simultaneous scheduling and control decisions in concentrated solar power (CSP) systems. Our algorithm is motivated by the need to determine optimal market participation strategies at multiple timescales. The decomposition scheme uses physical insights to create surrogate linear models that are embedded within a mixed-integer linear scheduling layer to perform discrete (operational mode) decisions. The schedules are then validated for physical feasibility in a dynamic optimization layer that uses a continuous full-resolution CSP model. The dynamic optimization layer updates the physical variables of the surrogate models to refine schedules. We demonstrate that performing this procedure recursively provides high-quality solutions of the simultaneous scheduling and control problem. We exploit these capabilities to analyze different market participation strategies and to explore the influence of key design variables on revenue. Our results also indicate that using scheduling algorithms that neglect detailed dynamics significantly decreases market revenues. © 2018 American Institute of Chemical Engineers *AIChE J*, 64: 2408–2417, 2018

Keywords: mixed integer programming, dynamic optimization, electricity markets, solar energy, thermal energy storage

Introduction

Electrical power infrastructures are being restructured to enable the adoption of intermittent solar and wind resources. Despite their environmental benefits, renewable sources introduce additional uncertainty over different timescales (seconds to seasonal). As a result, technologies that offer a broader spectrum of dynamic flexibility are becoming increasingly attractive. In particular, embedding energy storage technologies within generation systems such as concentrated solar power systems (CSP) is critical to ensuring security and reliability of power supply. Power grids use market-based mechanisms to coordinate electricity generation and consumption.[1–3] Operating CSP systems under such dynamic market environments is complicated because price dynamics are often out-of-phase with solar irradiance (which is the main energy source in such technologies). In California, for instance, average prices reach their minimum around noon and double to their maximum shortly after sunset.[4]

Recent literature considers direct participation of CSP systems in wholesale electricity markets.[5–9] Market revenues for CSP systems are estimated by solving a mixed integer linear programming (MILP) problems that incorporate market rules, CSP physics, and historical market prices and weather conditions. Integer variables are used to model transitions between different operating modes (e.g., generating mode, warm, off, antifreeze, and etc.).[8] To enable computational tractability, linear steady-state models that track only energy flows and holdups are often considered.[6] For example, a CSP market dispatch system based on MILPs was recently added to System Advisor Model (SAM), a ubiquitous software tool for techno-economic analysis of solar power systems.[10,11] Market participation of CSP systems, however, requires capturing the impact of weather and market price dynamics at high temporal resolution[5] to properly assess dynamic physical flexibility. In particular, dynamic models are needed to identify market opportunities at fast timescales (seconds to minutes), which are becoming increasingly profitable.[1] The controls community has used detailed dynamical models to capture nonlinear effects such as nonisothermal mixing and Rankine cycle efficiency.[12–15] Combining scheduling and control (dynamic optimization) models results in nonconvex mixed integer nonlinear programs (MINLPs) that cannot be solved by off-the-shelf solvers. Vasallo and Bravo[16,17] propose a two-model approach to address this issue; here, a MILP is solved to determine the optimal generation schedule which is then simulated with a high-fidelity dynamic model implemented in SAM.[10] The high-fidelity simulation results are then used to tune the optimization model. In this work, we propose an alternative framework where the high-fidelity simulation is replaced with a nonlinear dynamic optimization problem within the decomposition framework. We use physical insights to create a surrogate model for the scheduling layer that is progressively

Additional Supporting Information may be found in the online version of this article.

Current address of Alexander W. Dowling: Department of Chemical and Biomolecular Engineering, University of Notre Dame, IN, 46556.

Correspondence concerning this article should be addressed to V. M. Zavala at victor.zavala@wisc.edu.

refined by the dynamic optimization layer. We use this framework to address the following research questions:

1. What is the economic impact of neglecting dynamic physical flexibility in scheduling decisions?

2. Which market timescales and products offer the most revenue potential for CSP systems?

3. How are market revenues affected by design decisions such as solar collector and storage tank sizes?

The remainder of this paper is organized as follows. Section 2 reviews electricity markets and summarizes mathematical models for market participation. Section 3 describes a high-fidelity dynamic model for parabolic trough CSP systems. The proposed decomposition algorithm is presented in Section 4. Section 5 gives computational results and discussion. Conclusions and future work are discussed in Section 6. Nomenclature is defined and detailed mathematical models are given in the Supporting Information.

Electricity Market Participation Mechanisms

Electricity markets involve sophisticated hierarchical decision-making processes that coordinate generation and consumption in the power grid at multiple timescales. In North America, resources participate in markets by transacting two categories of products: electrical energy (measured in MWh) and ancillary service capacity (measured in MW). In California, *energy* is transacted at three timescales: in 1-h intervals in the Day-Ahead Market (DAM, also known as the Integrated Forward Market), in 15-min intervals in the Fifteen Minute Market (FMM), and in 5-min intervals in the Real Time Dispatch Process (RTD). Together, the FMM and RTD are known as the Real-Time Market (RTM). Figure 1 shows historical energy prices for seven days near Daggett, CA. Notably, prices are highest and most volatile in the evening. The lowest prices occur around midday, likely due to large amounts of distributed photovoltaic (PV) panels in CA. Significant price volatility can be observed in the RTM in the mornings, which corresponds to PV resources ramping up. Table 1 gives descriptive statistics for the entire year. Although the DAM prices are 1.4 to 1.5 $/MWh higher on average, the RTM prices are three to six times more volatile. These cyclic and volatile prices create significant incentives for energy storage. For CSP systems, up to 400,000 $/year of additional revenue are available by shifting 10 MW of generation from the average *real-time* energy price ($30/MWh) to the 1% most extreme prices (97 to 1621 $/MWh).[4] Computational results show how CSP systems can miss significant revenue opportunities without RTM participation.

Table 1. Descriptive Statistics for Wholesale Electricity Prices (in $/MWh) From Year 2015 Near Daggett, CA

	Mean	Standard Deviation
DAM	31.2	9.2
FFM	29.7	33.5
RTD	29.9	64.0
DAM minus FFM	1.5	25.0
DAM minus RTD	1.4	41.9

The last two rows correspond to the difference in *coincidental* prices between DAM and RTM layers. Data were obtained from oasis.caiso.com.

Besides conducting direct energy transactions, power generation technologies can also participate in electricity markets by providing *ancillary services* such as frequency regulation, spinning reserves, and nonspinning reserves. Ancillary services are a contingency product where resources are paid for providing a power capacity (prices are in $/MW). Reserve capacity is used as contingency against unplanned events that cannot be mitigated alone by RTM energy transactions, such as wind and solar supply variations, generator failures, and large errors in load forecasts. For example, a generator providing *spinning reserves* for CAISO is contractually obligated to fully respond within 10 min of dispatch and provide 30 to 60 min of power at the awarded capacity.[18] A resource providing reserves is paid both for the awarded capacity and then for energy provided during dispatch. Furthermore, reserve dispatches are rare and occur about fifty times per year.[19,20] As shown in the Results and Discussion section, spinning reserves are especially attractive for CSP systems where the steam turbines are typically idle. Moreover, with sufficient energy storage, a CSP system can operate in spinning mode (turbine is synchronized with the grid but not generating electricity) which both provides supplemental revenue for the generator and helps ensure grid reliability.

Frequency regulation (FR) is another important revenue opportunity for CSP systems. As the name implies, the FR ancillary service is used to help stabilize the AC power frequency of the grid (e.g., 60 Hz in North America, 50 Hz in Europe). FR capacity is bid to the market as a *flexibility band*. Every 2 to 15 seconds, the grid sends each participating resource a new power set-point within the awarded flexibility band. Resources are paid for both the size of the band, known as capacity payments, and the variability of the set-point signal, known as mileage payments. A CSP system providing 10 MW of FR capacity for all hours of 2015 in the California market would have received $500,000 in capacity payments alone.[4] To provide FR capacity, a resource must have sufficient fast dynamic flexibility on the order of seconds to minutes,

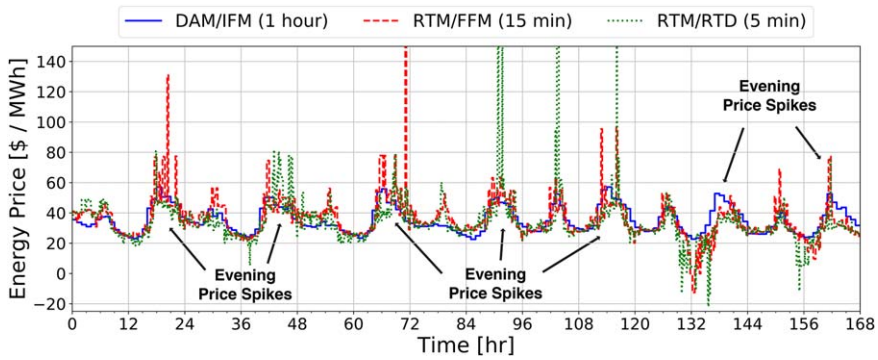

Figure 1. Energy prices near Daggett, CA from January 1st through 7th, 2015.

[Color figure can be viewed at wileyonlinelibrary.com]

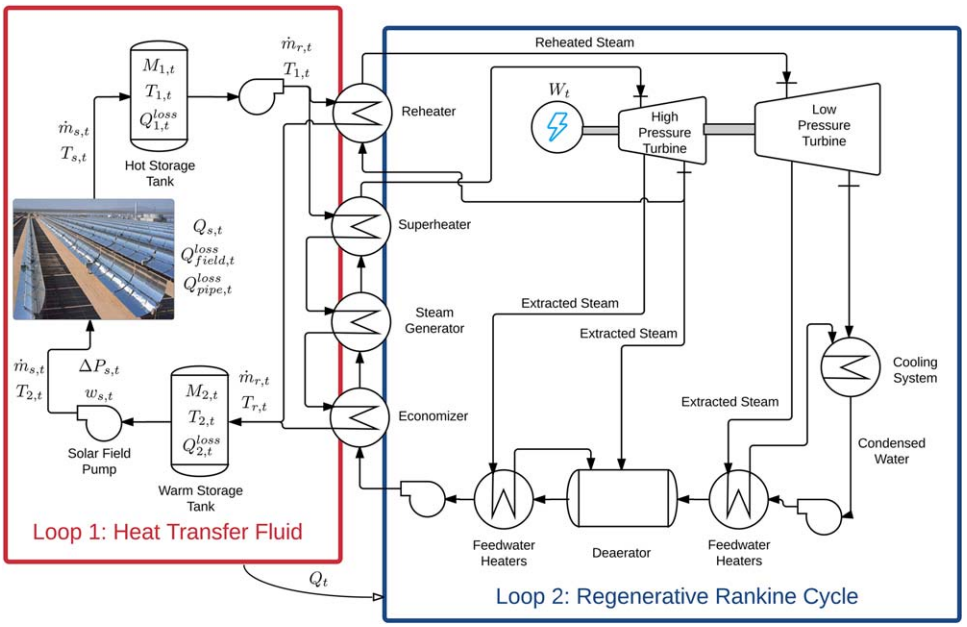

Figure 2. Parabolic trough CSP systems, modeled as two interconnected loops.

[Color figure can be viewed at wileyonlinelibrary.com]

which is why FR is the most expensive ancillary service. Dowling and Zavala[21] recently found that FR dispatch signals are predominantly composed of fast harmonics (seconds to hours) which are naturally attenuated by slow process dynamics. Thus, CSP systems should be able to provide frequency regulation by exploiting dynamic flexibility from thermal energy storage. Coal-fired generators, which are also based on Rankine cycles, have been providing FR capacity for decades.

A key challenge for market participants is to determine how to best allocate their generation capacity among market products and timescales. This is especially challenging given complex market rules, physical limitations of the technology, and multiscale correlations embedded in coincidental market prices and weather. As such, most existing market dispatch frameworks and techno-economic assessments for CSP systems, such as,[6–9,11] *focus solely on the day-ahead market or only energy transactions or both*. Dowling et.al.[1] recently proposed an optimization framework to identify optimal participation strategies in *multiscale and multiproduct electricity markets*. Their modeling abstraction is general purpose and can be coupled to detailed physical models of different technologies. We now proceed by describing the basic components of the market participation model. For more details, the reader is referred to.[1]

We define the sets of *time intervals* $\mathcal{T}_\ell := \{1, \ldots, N_\ell\}$ where ℓ indicates the market layer and $\ell \in \mathcal{L} := \{3, 2, 1, 0\}$ and Δt_ℓ denotes the length of the time interval in layer $\ell \in \mathcal{L}$ (units of hours). For markets in CAISO, $N_1 = 24$ ($\Delta t_1 = 1$ h), $N_2 = 4$ ($\Delta t_2 = 15$ min), and $N_3 = 3$ ($\Delta t_3 = 5$ min). The lexicographic time set

$$\begin{aligned}\mathcal{T}^* :=& \mathcal{T}_{|\mathcal{L}|} \times \cdots \times \mathcal{T}_2 \times \mathcal{T}_1 \times \mathcal{T}_0 \\ =& \{(1,1,1,1),(2,1,1,1),\ldots,(N_3,1,1,1),(1,2,1,1),\ldots, \\ & (N_3,N_2,1,1),\ldots,(N_3,N_2,N_1,N_0)\}\end{aligned} \tag{1}$$

captures the hierarchical nature of the time discretization. Lexicographic time sets for individual layers are similarly defined: $\mathcal{T}_3^* := \mathcal{T}^*$, $\mathcal{T}_2^* := \mathcal{T}_2 \times \mathcal{T}_1 \times \mathcal{T}_0$, $\mathcal{T}_1^* := \mathcal{T}_1 \times \mathcal{T}_0$, and $\mathcal{T}_0^* = \mathcal{T}_0$. Thus, an instance in time t is defined by the tuple (i_3, i_2, i_1, i_0) such that $(i_3, i_2, i_1, i_0) \in \mathcal{T}_3$, $(i_2, i_1, i_0) \in \mathcal{T}_2$, and so forth. We use $\overline{E}_{\ell,t}$ and $\underline{E}_{\ell,t}$ for $t \in \mathcal{T}_\ell$ to represent the energy sales and purchases, respectively, for market layer ℓ. Similarly, we use $A_{a,\ell,t}$ to represent ancillary service capacity sales, where $a \in \mathcal{A} := \{s, n, r^+, r^-\}$ (for spinning reserves, nonspinning reserves, regulation up, and regulation down). The total market revenues, denoted by R, are calculated as follows

$$R = \Lambda \sum_{\ell \in \mathcal{L}} \sum_{t \in \mathcal{T}_\ell} \left[\Delta_t \pi^E_{\ell,t} \left(\overline{E}_{\ell,t} - (1+\epsilon_\pi) \underline{E}_{\ell,t} \right) + \sum_{a \in \mathcal{A}} \pi^A_{a,\ell,t} A_{a,\ell,t} \right] \tag{2}$$

where π^E and π^A are the time-vary prices for energy and ancillary service capacity, ϵ_π is a small number (e.g., 10^{-6}), and Λ is the nameplate capacity of the generator. We use E_t to represent the net energy flow out of the energy system which is defined at the fastest timescale as follows

$$E_t = \hat{E}_t + \sum_{\ell \in \mathcal{L}} \left(\overline{E}_{\ell,t} - \underline{E}_{\ell,t} \right), \quad t \in \mathcal{T}^* \tag{3}$$

where $\hat{E}_t$ represents the flow of energy to onsite demands (such as pumps and other auxiliary loads). Under this basic market participation abstraction, the detailed energy systems model only needs to interface with variables E_t and $\hat{E}_t$. All energy and ancillary service capacity variables are scaled by the nameplate capacity, denoted by Λ, such that $0 \le E_t, \hat{E}_t, \overline{E}_{\ell,t}, \underline{E}_{\ell,t}, A_{a,\ell,t} \le 1$. A 3% per minute ramp rate restriction is imposed on E_t in the market model (see[1]) which is consistent with the ramping limits for other Rankine cycles.[22]

Mathematical Model and Optimization Formulation

CSP systems transform thermal energy collected from the sun into electricity. As show in Figure 2, CSP systems are

organized into two interconnected loops. In Loop 1, an advanced organic heat-transfer fluid (HTF) such as Dowtherm A* is heated in the parabolic trough solar collectors and stored in the hot storage tank. When the CSP system generates electricity, the hot HTF is pumped into the warm storage tank via heat exchangers. Heat is transferred from Loop 1 into Loop 2, which is a standard regenerative Rankine cycle. This configuration allows for energy collection and conversion to be partially decoupled such that electricity generation can occur during times with low solar irradiance. This configuration, however, introduces control challenges for CSP systems. In particular, it is necessary to coordinate mass and energy hold-ups in the storage system while ensuring operational restrictions of the individual loops.[23]

Strategic market participation for CSP systems can be formulated as the following mixed integer dynamic optimization problem

$$\max_{z(t),x(t),u(t),y(t)} \int_0^{T_f} \pi^T u(t)\,dt \tag{P1a}$$

$$\text{s.t.} \quad Au(t)+By(t) \le 0 \tag{P1b}$$

$$\frac{dz}{dt}=f(z(t),x(t),u(t)) \tag{P1c}$$

$$g(z(t),x(t),u(t))=0 \tag{P1d}$$

$$\underline{z} \le z(t) \le \bar{z} \tag{P1e}$$

$$\underline{x} \le x(t) \le \bar{x} \tag{P1f}$$

$$\underline{u} \le u(t) \le \bar{u} \tag{P1g}$$

where $z(t) \in \mathbb{R}^{n_z}$ are differential states, $x(t) \in \mathbb{R}^{n_x}$ are algebraic states, $u(t) \in \mathbb{R}^{n_u}$ are continuous control variables, and $y(t) \in \{0,1\}^{n_y}$ are discrete control variables. The most important variables in the CSP mathematical model are shown in Figure 2. Differential states track the time-evolution of mass ($M_{1,t}$, $M_{2,t}$) and temperature ($T_{1,t}$, $T_{2,t}$) in thermal storages tanks 1 and 2. Algebraic states include the gross power output of the turbines (W_t) as well as HTF temperature leaving the solar collector field ($T_{s,t}$) and Rankine cycle ($T_{r,t}$); these are calculated from algebraic performance correlations.[24] Continuous control variables include HTF mass flow rates through the solar collectors ($\dot{m}_{s,t}$) and Rankine cycle ($\dot{m}_{r,s}$) as well as capacity allocation to market products ($\bar{E}_{\ell,t}$, $A_{a,\ell,t}$, etc). Finally, discrete control variables $y_{e,t}$ and $y_{sp,t}$, describe if the CSP system is in ON, SPIN, or OFF modes.

The objective function of (P1) is often to maximize revenue, as given in (2). The market rules (described in[1]) and operation restrictions are modeled linear constraints (P2b). Mass and energy balances for the storage tanks give rise to the nonlinear differential equations (P2c). Similarly, nonlinear performance correlations for the solar collectors and Rankine cycle comprise the algebraic constraints (P2d). Finally, the differential and algebraic states are subject to path constraints (bounds). The complete CSP physics model is reported in the Supporting Information.

Problem (P1) is discretized with a 5-min timestep, which corresponds with the fastest market layer, resulting in a complex nonconvex Mixed Integer Nonlinear Problem (MINLP). For example, with a scheduling horizon of only one day, (P1) contains 8250 continuous variables, 72 binary variables, 9036 linear constraints, and 2916 nonlinear constraints. About 20% of the continuous variables and 30% of the linear constraints arise from the market participation model. Despite the fact that this is an MINLP of moderate size, the off-the-shelf global solver SCIP 4.0 often did not advance beyond the initial point and occasionally failed to compute valid bounds. Bonmin was unable to solve (P1) for planning horizons longer than three days (see Computational Results section).

*http://www.dow.com/heattrans/csp/index.htm

Decomposition Algorithm

In order for (P1) to be used for daily market participation decisions, it needs to be solved in less than a few hours for a multiday planning horizons. To meet this computational budget, we propose a decomposition algorithm, which we refer to as (AR1)

Decomposition algorithm (AR1).

Data: Market prices, solar irradiance, and other model parameters
for $k = 1$ ***to*** N **do**
  if $k = 1$ **then**
    Load data and assemble (P2.1)
    Solve (P2.1) and store results in $v^*_{2,k}$
  else
    Assemble (P2.2) using results $v^*_{3,k-1}$
    Solve (P2.2) and store results in $v^*_{3,k}$
  End
  Fix discrete variables at values in $v^*_{2,k}$
  Simulate CSP system using $v^*_{2,k}$ and initialize (P3)
  Solve (P3) and store results in $v^*_{3,k}$
  Merge $v^*_{2,k}$ and $v^*_{3,k}$ to form $v^*_{1,k}$, a feasible solution for (P1)
end

The key insight in (AR1) is to decompose the full problem (P1), and iterate between scheduling optimization problems (P2) and nonlinear dynamic optimization problems (P3). Two formulations for the scheduling problem as considered: formulation (P2.1) is used for initialization and formulation (P2.2) is used for subsequent iterations. Both formulations are given in the Supporting Information. The solution of (P2), which is stored in $v^*_{2,k}$, contains the time trajectory for the discrete operating mode decisions $y_{e,t}$ and $y_{sp,t}$ (these have a time resolution of one hour). These variables are fixed for in the dynamic optimization problem (P3), which contains the full-resolution CSP physics with 5-min time discretization (this corresponds to the faster CAISO market layer). For each subsequent iteration of (AG1), the surrogate model used in (P2) is updated based on the solution of (P3) from the previous iteration (which is contained in $v^*_{3,k-1}$). The proposed decomposition approach has the advantage that (P2) and (P3) can be solved with off-the-shelf solvers. Moreover, the surrogate physical models used in (P2) are constructed to be consistent with (P3), which leads to favorable numerical results. The remainder of this section details the formulations for (P2) and (P3).

Scheduling Problem

The goal of problem (P2) is to compute schedule operational modes. To accomplish this, the full-resolution CSP

physics model is simplified into linear constraints, $\hat{f}(\cdot)$ and $\hat{g}(\cdot)$, to create a surrogate model

$$\max_{\hat{z}(t),x(t),u(t),y(t)} \int_0^{T_f} \pi^T u(t)\,dt \tag{P2a}$$

$$\text{s.t.} \quad Au(t)+By(t) \le 0 \tag{P2b}$$

$$\frac{d\hat{z}}{dt}=\hat{f}(\hat{z}(t),x(t),u(t)) \tag{P2c}$$

$$\hat{g}(\hat{z}(t),x(t),u(t))=0 \tag{P2d}$$

$$\underline{\hat{z}} \le \hat{z}(t) \le \bar{\hat{z}} \tag{P2e}$$

$$\underline{x} \le x(t) \le \bar{x} \tag{P2f}$$

$$\underline{u} \le u(t) \le \bar{u} \tag{P2g}$$

We propose a tailored linearization from $f(\cdot)$ and $g(\cdot)$. In the full-resolution model, storage tank variables are differential states, that is, $z(t)=[M_1,M_2,T_1,T_2]^T$, which introduces bilinear terms in the energy balances

$$E_{i,t}=C_p M_{i,t} T_{i,t}, \tag{4}$$

where C_p is the heat capacity. In contrast, energy holdups in the storage tanks, E_1 and E_2, replace temperatures as state variable in simplified physical model, that is, $\hat{z}(t)=[M_1,M_2,E_1,E_2]^T$. As consequence of this change of basis, mass, and energy balances become linear. This is a key distinction from MINLP algorithms such as Outer Approximation,[25] which do not rely on physical insights to construct linearization. Moreover, the proposed algorithm updates the linearizations $\hat{f}(\cdot)$ and $\hat{g}(\cdot)$ each iteration and does not, at present, use information from previous iterations (besides the most recent). In contrast, Outer Approximation (and similar algorithms) accumulates information from all iterations as cutting planes in the master problem.

We observe that temperature dynamics are slow with sufficiently large storage tanks, and thus, (4) can be approximated as follows

$$M_{i,t}\,(\tilde{T}_{i,t}^{avg}-\delta_T) \le E_{i,t}\; C_p^{-1}\; \zeta_{kJ}^{MWh}\; \zeta_{\text{tonne}}^{kg} \le M_{i,t}\,(\tilde{T}_{i,t}^{\text{avg}}+\delta_T), \quad i \in \{1,2\} \tag{5}$$

where $\tilde{T}_{i,t}$ which represents the temperature in tank i at time t from the solution of (P3) at iteration k–1. We will use the notation $\tilde{x}$ to denote fixed values for variable x obtained from (P3) at iteration k–1. Linear Eq. 5 couple mass and energy holdup state variables and ensure the new solution of (P2) is in a neighborhood near the previous solution of (P3) (i.e., where the simplified model is still valid). δ_T is a tunable trust-region parameter that balances the accuracy of the simplified model and the exploration space allowed.[26]

The proposed approach has *two key distinctions* from other MILP models in literature:

1. Mass flows and holdups are considered in addition to energy flows and energy holdups. Other simplified models in the literature only consider energy holdups.

2. A 5-min timestep is used to match the fastest market layer, whereas most simplified models from literature use a 1-h timestep.

These distinctions ensure that the proposed surrogate model is consistent with the full-resolution model. In particular, the surrogate model is constructed such that any feasible solution of (P3) must be feasible solution to the next instance of (P2). In practice, solutions of (P2) often give good starting points for (P3), although, we cannot guarantee a feasible solution for (P3) for every set of discrete variables generated by (P2).

Dynamic Optimization Problem

The goal of the dynamic optimization problem (P3) is to find the optimal market participation and dispatch decisions for mass and energy flows for a fixed operating mode schedule obtained with (P2). This is formulated as follows,

$$\max_{z(t),x(t),u(t)} \int_0^{T_f} \pi^T u(t)\,dt \tag{P3a}$$

$$\text{s.t.} \quad Au(t)+By(t) \le 0 \tag{P3b}$$

$$\frac{dz}{dt}=f(z(t),x(t),u(t)) \tag{P3c}$$

$$g(z(t),x(t),u(t))=0 \tag{P3d}$$

$$\underline{z} \le z(t) \le \bar{z} \tag{P3e}$$

$$\underline{x} \le x(t) \le \bar{x} \tag{P3f}$$

$$\underline{u} \le u(t) \le \bar{u} \tag{P3g}$$

where $y(t)$ is fixed. Problem (P3) is discretized with a 5-min timestep resulting in a nonconvex nonlinear program (NLP).

Results and Discussion

In this section, we present computational results and use the proposed decomposition algorithm quantify the revenue potential of CSP systems from different market layers and products. We also use the algorithm to explore effect of design variables on revenue potential.

Computational performance

Algorithm (AR1) was used to optimize the market participation strategy for a parabolic trough system interacting in the California market. Problem (P2) was solved with Gurobi 7.0.2[27]with a MIP gap of 0.5% and (P3) was solved with Ipopt 3.12.4[28] using the MA27 linear algebra routines.[29] Historical market prices and weather data were obtained from oasis.caiso.com and UNLV,[30] respectively, for January 1–7, 2015. We note that the revenue estimates reported herein are upper bounds, as we assume exact forecasts. We will consider uncertainty as future work and note that Sioshansi and Denholm[31] report obtaining over 90% of available DAM revenues with simple forecasting strategies. The CSP model is based on the work of Patnode[24] and comprises a 35 MW_e net CSP generator. As a reference, the world's largest CSP plant, Ivanpah Solar, is 10 times larger.[†] For the seven-day planning horizon under study, (P2.2) contained approximately 39,000 continuous variables, 500 binary variables, and 75,000 linear constraints. Problem (P3) contained approximately 64,000 continuous variables, 37,000 linear constraints, and 18,000 nonlinear constrains. The decomposition algorithm was implemented in the Julia programming language using the JuMP modeling environment.[32,33]

The first case study explores evolution of the objective function (the total revenue) for 25 iterations of (AG1). Figures 3 and 4 present the revenue and computational times, respectively, with trust-region parameters $\delta_T=$ 10°C and 30°C. Table 2 reports results for $\delta_T=$ 1°C, 15°C, 20°C, 25°C, and 100°C too. From these results, we can draw the following conclusions:

- With $\delta_T=$10°C and 30°C, the revenue obtained with the scheduling model (P2) is about half of the best revenue

[†]http://www.nrel.gov/csp/solarpaces/

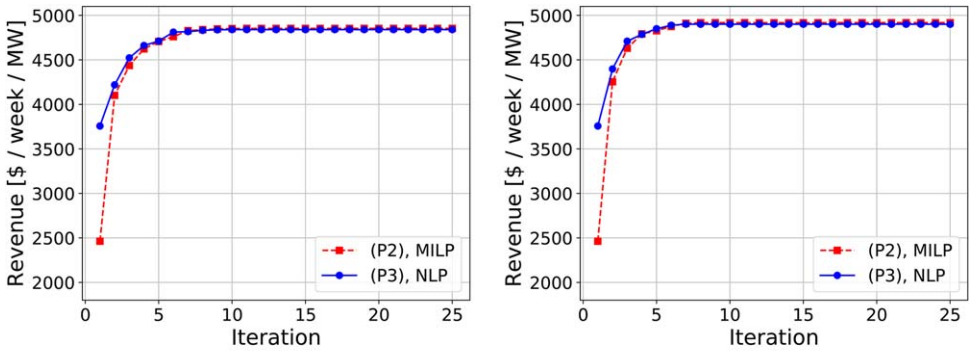

(a) $\delta_T = 10\ ^\circ\mathrm{C}$ (b) $\delta_T = 30\ ^\circ\mathrm{C}$

Figure 3. Revenues for (P2) and (P3) over 25 iterations.

(a) $\delta_T = 10\ ^\circ$C; (b) $\delta_T = 30\ ^\circ$C [Color figure can be viewed at wileyonlinelibrary.com]

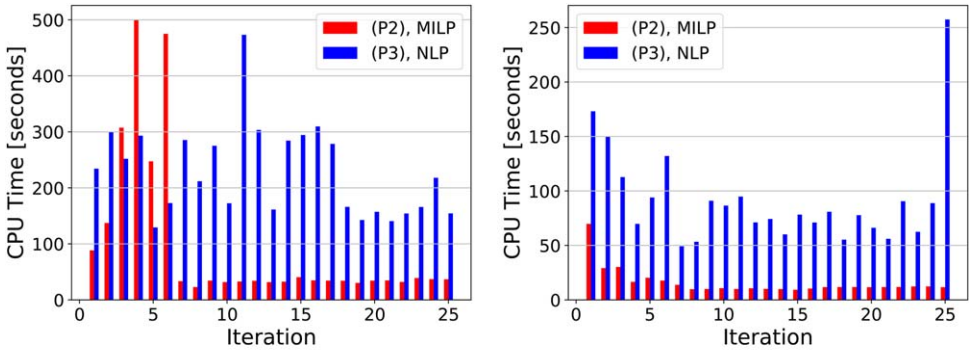

(a) $\delta_T = 10\ ^\circ\mathrm{C}$ (b) $\delta_T = 30\ ^\circ\mathrm{C}$

Figure 4. Computational times for (P2) and (P3) over 25 iterations.

(a) $\delta_T = 10\ ^\circ$C; (b) $\delta_T = 30\ ^\circ$C [Color figure can be viewed at wileyonlinelibrary.com]

obtained. This implies that the original surrogate CSP model used in the scheduling model poorly captures the dynamic flexibility of the CSP system.

- The algorithm (AG1) progressively improves the revenue and eventually settles. In particular, the revenue of (P3) is improved by nearly 35% (relative to the first iteration). We also note that the gap in revenue between the scheduling (P2) and dynamic optimization (P3) models eventually dies out.
- The trust-region parameter δ_T balances the rate of convergence, computational times, and the best revenue (objective) value. From Figure 3, (AG1) converges in about 8 iterations with both $\delta_T = 10\ ^\circ$C and $\delta_T = 30\ ^\circ$C. At the extreme $\delta_T = 1\ ^\circ$C, (AR1) converged after only two iterations to a local solution that only captures 77% of the available revenue. Table 2 shows that, in general, as δ_T increases, the computational demands also increase and shift from (P2) to (P3).
- For a given iteration, the objective values for (P3) are better than those of (P2). This highlights that (P2) is not a relaxation of (P3) but instead a linearization (approximation). Moreover, in early iterations the linear model in (P2) underpredicts revenue and missing opportunities only available from exploit dynamics and nonlinear effects.

We hypothesize the scheduling decisions are near optimal because the linear surrogate models $\hat{f}(\cdot)$ and $\hat{g}(\cdot)$ locally approximate the full-resolution dynamic model. This was tested by solving (P1), discretized with 5-min timesteps, using the four MINLP algorithms available with Bonmin.[25,34,35] The solution for (AR1) was used as an initial point for each instance solved with Bonmin. The results are shown in Table 3. We highlight that all of the solutions obtained with (AR1) were within 2% of best objective found with Bonmin, and for half of the instances, the difference was less than 0.5%. Algorithm (AR1) is 3 to 300 times faster than Bonmin. We note that Bonmin was unable to solve for planning horizons longer than 3 days, whereas (AR1) has been demonstrated with 7-day planning horizons (Figures 5–7). We hypothesize (AR1) is more computationally efficient because the linearization strategy exploits physicals insights for the system, where Bonmin is a general purpose MINLP solver. Algorithm (AR1) is not guaranteed to provide an optimal solution but in practice it can

Table 2. Revenues and Computational Times for (P2) and (P3) Over 25 Iterations

δ_T	Revenue	Total Time for (P2)	Total Time for (P3)
1 °C	3757 $/week	0.6 CPU-hours	0.3 CPU-hours
10 °C	4840 $/week	0.7 CPU-hours	1.6 CPU-hours
15 °C	4851 $/week	0.3 CPU-hours	6.1 CPU-hours
20 °C	4882 $/week	0.1 CPU-hours	2.7 CPU-hours
25 °C	4876 $/week	0.2 CPU-hours	1.2 CPU-hours
30 °C	4901 $/week	0.1 CPU-hours	0.6 CPU-hours
100 °C	4885 $/week	0.1 CPU-hours	1.7 CPU-hours

Table 3. Comparison of (AR1) with Settings $\delta_T = 30$ °C and 10 Iterations and Four Algorithms in Bonmin: B-BB is Branch-and-Bound, B-QG is Branch-and-Cut,[35] B-OA is Outer Approximation,[25] and B-Hyb is a Hybrid Strategy

Market Products	Horizon	Algorithm	Objective	CPU-Time
Energy Only	1 day	(AR1)	$621.4	44.3 s
		B-BB	$621.4	271.1 s
		B-QG	$621.4	111.7 s
		B-Hyb	$621.4	71.6 s
		B-OA	$589.8	15,976.0 s
Energy Only	2 days	(AR1)	$1231.5	131.5 s
		B-BB	$1256.5	21,656.9 s
		B-QG	$1255.4	3611.7 s
		B-Hyb	$1191.0	3229.3 s
Energy Only	3 day	(AR1)	$1869.1	333.3 s
		B-BB	$1783.2	21,760.6 s
		B-QG	$1886.3	22,036.7 s
		B-Hyb	$1896.4	7159.1 s
All Products	1 day	(AR1)	$670.9	31.7 s
		B-BB	$671.1	989.4 s
		B-QG	$671.1	142.4 s
		B-Hyb	$671.1	244.9 s
All Products	2 days	(AR1)	$1369.8	129.5 s
		B-BB	$1366.6	21,646.4 s
		B-QG	$1373.2	21,780.5 s
		B-Hyb	$1369.2	4,543.8 s

All five algorithms were tried for each instance. Omitted rows indicate failure to find a feasible solution within 8 h.

be used to obtained feasible solutions of good quality. We will study the convergence properties as part of future work.

Market Participation

In a second case study, we used algorithm (AR1) to quantify the revenue opportunities from different market products and timescales. Figure 5 compares twelve different market participation strategies, organized into three groups: participation in both markets, only the day-ahead market, and only the real-time market. Four combinations of market products are considered for each group: (a) energy only, (b) energy and regulation, (c) energy and spinning reserves, and (d) energy, regulation and spinning reserves. The pattern in each bar denotes the total revenue from each timescale. Revenues are extrapolated to one year for a better sense of scale. We draw the following conclusions:

- Market participation in day-ahead markets only captures 60% (energy and ancillary services) to 70% (energy only) of the available revenue obtained from participation in both markets. In contrast, participating in the real-time market alone captures over 85% of the available revenues. This highlights the importance of fast flexibility and the need to consider dynamic models in scheduling decisions.
- Ancillary services offer substantial new revenue streams for CSP systems: up to 50% (DAM), 30% (RTM), and 29% (both) revenue improvements are obtained relative to energy-only market participation.
- For DAM participation, spinning reserves are the most valuable ancillary service, increasing revenues 30% relative to energy only participation. These results are in agreement with,[6] who found a 17% increase in revenue from spinning reserves. However, when participating in the RTM or both markets, regulation is the most valuable ancillary service.

We now examine the operational policies obtained for full market participation (for all products and timescales) in more detail to elucidate how the CSP system exploits dynamic flexibility to maximize revenues. Figure 6a gives the optimal allocation of generation capacity into market products. Energy sales are show in purple (with cross pattern) with the average generation level marked with the solid black line. Regulation up and down capacity are shown in red and blue, respectively. Recall that regulation is an ancillary service where the generator provides a flexibility band. This means that the actual energy production will be between the bottom of the blue region (reg. down) and the top of the red region (reg. up). Careful inspection reveals that the regulation down capacity (blue) overall with some of the energy sales (purple). Finally, spinning reserve capacity is shown in green. Figure 6b shows the optimal control strategy, including the two primary energy flows, collection of solar heat and electricity generation, as well as energy levels in the hot and warm storage tanks. From Figure 6, we draw the following conclusions:

- Optimal energy sales often correspond to periods of high prices (see Figure 1), in particular during the morning and evening. Energy is sometimes sold during times of medium or low prices to help manage the mass and energy holdup in the storage tanks.
- Energy sales are always paired with selling regulation capacity. When the regulation down capacity price is higher than the up-capacity price, it is optimal to set nominal generation between 90% and 100% and sell a 20 to 30% regulation down capacity. Similarly, when regulation up is more expensive, it is optimal to set nominal generation between 60% and 70% and sell the remaining capacity as regulation up. Likewise, spinning reserve prices are sometimes higher than and displace regulation up capacity sales.
- Spinning reserves allow CSP systems to capture revenue when they would otherwise be off. This occurs only a few times during the 7-day horizon shown in Figure 6a. This is because, for these results, assume operating in spinning mode incurs an energy penalty of 5% of the nameplate capacity ($\xi = 0.05$, see Supplemental Information). When spinning mode losses are not considered ($\xi = 0$, see[36]) spinning reserves are almost always sold instead transitioning into off mode. Detailed modeling to determine the energy losses in spinning mode is beyond the scope of this work.

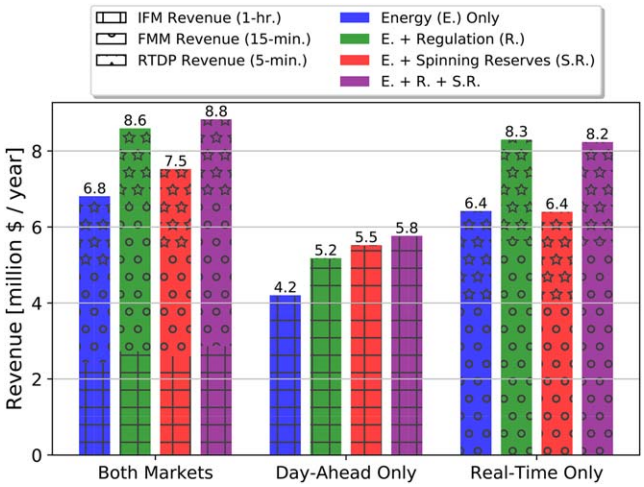

Figure 5. Comparison of revenue streams from different market participation strategies.

(a) Market participation schedule; (b) Energy flows and holdups [Color figure can be viewed at wileyonlinelibrary.com]

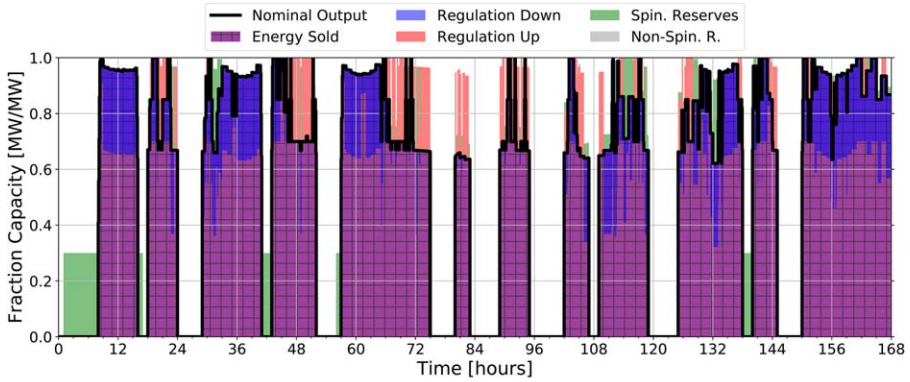

(a) Market participation schedule

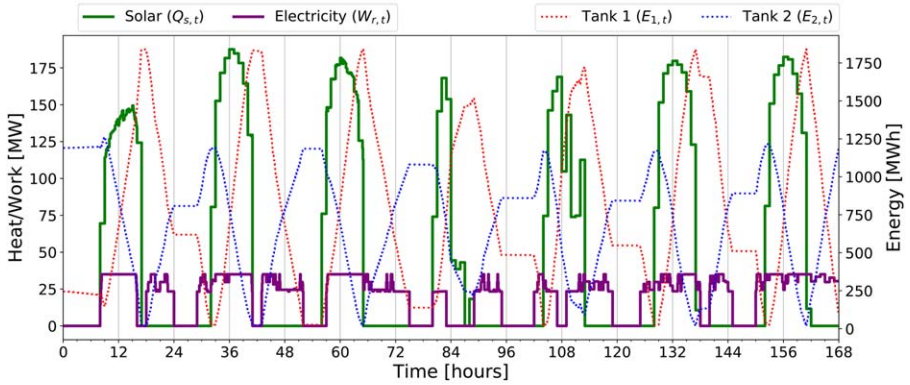

(b) Energy flows and holdups

Figure 6. Optimal market participation schedule and energy flows for January 1–7, 2015.

(a) Solar field size; (b) Thermal storage size [Color figure can be viewed at wileyonlinelibrary.com]

• The hot tank storage is almost completely emptied of useful energy each night, suggesting there is little coupling between days. This aligns with the observations of,[21] where the authors found that most market volatility and hence revenue opportunities are intraday.

Effects of Design

The third and final case study examines the impact of two design decisions, solar field size and storage tank size, on market revenues. In this study, all market timescales are considered and we vary the type of products provided. The nominal configuration was a solar multiple (Θ) of 1.5 with 8 h of thermal storage (output at full nameplate capacity), which was used for the previous results. Figure 7 shows sensitivity analysis results around this nominal design for these market participation strategies. Absolute revenues (extrapolated to one full year) are shown for the energy only case. The relative increases in revenue are reported for all other product combinations. We make the following observations:

• For some trials in the solar multiple sensitivity analysis, such as Θ=1.75 (E + R + SR), Θ=2.0 (E + SR, E + R), Θ

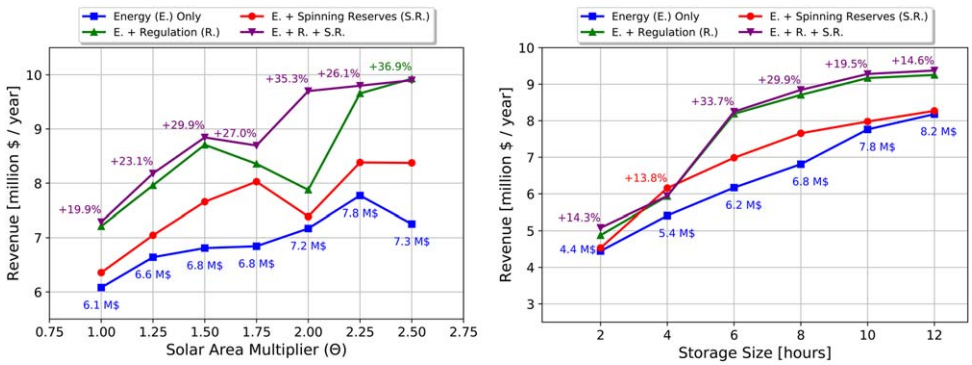

(a) Solar field size

(b) Thermal storage size

Figure 7. Sensitivity of market revenues to perturbations in design parameters.

[Color figure can be viewed at wileyonlinelibrary.com]

$=2.5$ (E, E + SR), revenues are less than overall trends. It is likely that for these points (AR1) found solutions that are not globally optimal.

- With energy-only participation, revenues flatten out for solar multiples above 1.5. With simultaneous energy and ancillary service sales, however, revenues do not flatten out and continue to increase as the solar multiple increases.
- Over the solar field sizes considered, full market participation increased revenues 20% to 37% over energy only participation. Similarly, ancillary services increased revenues 14% to 34% over the range of storage sizes considered.
- Revenues almost doubled over the range of storage sizes considered: from 4.4 M$/yr with 2 h of storage to 8.2 M$/yr with 12 h of storage (energy only). Gains from varying the doubling the solar field size were more modest.

Conclusions and Future Work

We present a computationally efficient decomposition algorithm to perform simultaneous scheduling and control decisions in CSP systems. Physical insights inform an embedded, tunable surrogate linear model that couples mixed-integer linear scheduling layer and a dynamic optimization layer. With this algorithm, we find dramatic revenue opportunities for CSP systems participating in multiscale electricity markets. We show how up to 40% of revenue opportunities are only accessible through the real-time market, yet most literature neglects these fast timescales. We also find that selling ancillary service capacity can increase market revenues up to 50%. As such, advanced control strategies and market participation offers CSP technologies means to improve their *value proposition* relative to other renewable technologies *without dramatic increases in capital costs*.

As future work, we plan to consider design and market participation co-optimization[37,38] as well as probabilistic weather and price forecasts.[9,39–42] Yet modeling multiscale effects (minutes to decades) and uncertainty often result in extremely large optimization problems. To address the computation challenges, we propose exploiting problem structure and using massively parallel optimization solvers such as[43,44] for the subproblems (P2) and (P3). We also plan to apply this decomposition algorithm to other chemical processes and thermal energy storage systems.

Acknowledgments

The authors thank The Dow Chemical Company for their generous financial support. This contribution was identified by Wesley Cole (National Renewable Energy Laboratory, Golden, CO, USA) as the *Best Presentation* in the session "Sustainable Electricity: Generation and Storage" of the 2016 AIChE Annual Meeting in San Francisco. Finally, we would like to thank two anonymous reviewers for their constructive comments and suggested improvements.

Literature Cited

1. Dowling AW, Kumar R, Zavala VM. A multi-scale optimization framework for electricity market participation. *Appl Energy*. 2017; 190:147–164.
2. Chmielewski D. Smart grid: the basics—what? why? who? how? *CEP Mag*. 2014;(Aug):28–34. Available at https://www.aiche.org/resources/publications/cep/2014/august/special-section-energy-smart-grid-basics-what-why-who-how
3. Wang Q, Zhang C, Ding Y, Xydis G, Wang J, Østergaard J. Review of real-time electricity markets for integrating distributed energy resources and demand response. *Appl Energy*. 2015;138:695–706.
4. Dowling AW, Zheng T, Zavala VM. Economic assessment of concentrated solar power technologies: a review. *Renew Sust Energy Rev*. 2017;72:1019–1032.
5. Lizarraga-Garcia E, Ghobeity A, Totten M, Mitsos A. Optimal operation of a solar-thermal power plant with energy storage and electricity buy-back from grid. *Energy*. 2013;51:61–70.
6. Madaeni SH, Sioshansi R, Denholm P. How thermal energy storage enhances the economic viability of concentrating solar power. *Proceed IEEE*. 2012;100(2):335–347.
7. Usaola J. Operation of concentrating solar power plants with storage in spot electricity markets. *IET Renew Power Gen*. 2012;6(1):59–66.
8. González JL, Dimoulkas I, Amelin M. Operation planning of a CSP Plant in the Spanish day-ahead electricity market. In: *11th International Conference on the European Energy Market (EEM)*, Krakow, Poland. 2014:1–5. Available at http://ieeexplore.ieee.org/document/6861303/
9. Dominguez R, Baringo L, Conejo A. Optimal offering strategy for a concentrating solar power plant. *Appl Energy*. 2012;98:316–325.
10. Dobos A, Gilman P. System advisor model. Technical report, National Renewable Energy Laboratory. NREL Report No. TP-6A20–53437, 2012.
11. Wagner MJ, Newman AM, Hamilton WT, Braun RJ. Optimized dispatch in a first-principles concentrating solar power production model. *Appl Energy*. 2017;203:959–971.
12. Powell KM, Edgar TF. Modeling and control of a solar thermal power plant with thermal energy storage. *Chem Eng Sci*. 2012;71:138–145.
13. Powell KM, Hedengren JD, Edgar TF. Dynamic optimization of a hybrid solar thermal and fossil fuel system. *Solar Energy*. 2014;108:210–218.
14. Camacho EF, Gallego AJ. Optimal operation in solar trough plants: a case study. *Solar Energy*. 2013;95:106–117.
15. Ghobeity A, Mitsos A. Optimal design and operation of a solar energy receiver and storage. *J Solar Energy Eng*. 2012;134(3):031005.
16. Vasallo MJ, Bravo JM. A novel two-model based approach for optimal scheduling in CSP plants. *Solar Energy*. 2016;126:73–92.
17. Vasallo MJ, Bravo JM. A MPC approach for optimal generation scheduling in CSP plants. *Appl Energy*. 2016;165:357–370.
18. CAISO fifth replacement FERC electric tariff, 2015. Available at www.caiso.com
19. Todd D, Caufield M, Helms B, Starke M, Kirby B, Kueck J. Providing reliability services through demand response: a preliminary evaluation of the demand response capabilities of Alcoa Inc. Technical report, Alcoa Power Generating, Inc; Oak Ridge National Laboratory, 2009. ORNL/TM-2008/233.
20. Todd D. They said it couldnt be done: Alcoas experience in demand response. In *Texas Industrial Energy Management Forum: Energy Management in the Age of Shale Gas*, Houston, TX, 2013.
21. Dowling AW, Zavala VM. Economic opportunities for industrial systems from frequency regulation markets. *Comput Chem Eng*. In press. https://doi.org/10.1016/j.compchemeng.2017.09.018
22. Bai X, Clark K, Jordan GA, Miller NW, Piwko RJ. Intermittency analysis project: appendix B—impact of intermittent generation on operation of California power grid. Technical report, California Energy Commission/GE Energy Consulting, 2007.
23. Zhang H, Baeyens J, Degrève J, Cacères G. Concentrated solar power plants: Review and design methodology. *Renew Sust Energy Rev*. 2013;22:466–481.
24. Patnode AM. *Simulation and Performance Evaluation of Parabolic Trough Solar Power Plants*. Masters of Science, University of Wisconsin-Madison, Madison, WI, 2006.
25. Duran MA, Grossmann IE. An outer-approximation algorithm for a class of mixed-integer nonlinear programs. *Math Program*. 1986; 36(3):307–339.
26. Conn AR, Gould NI, Toint PL. *Trust Region Methods*. SIAM, 2000.
27. G. O. Inc. Gurobi optimizer reference manual, Houston, TX, 2016.
28. Wächter A, Biegler TL. On the implementation of an interior-point filter line-search algorithm for large-scale nonlinear programming. *Math Program*. 2006;106(1):25–57.
29. HSL. A collection of Fortran codes for large scale scientific computation.
30. Andreas A, Stoffel T. Technical report, University of Nevada (UNLV), NREL Report No. DA-5500–56509, 2006. http://dx.doi.org/10.5439/1052548
31. Sioshansi R, Denholm P. The value of concentrating solar power and thermal energy storage. *IEEE Trans Sust Energy*. 2010;1(3):173–183.
32. Bezanson J, Edelman A, Karpinski S, Shah VB. Julia: a fresh approach to numerical computing. *SIAM Rev*. 2017;59(1):65–98.
33. Dunning I, Huchette J, Lubin M. Jump: a modeling language for mathematical optimization. *SIAM Rev*. 2017;59(2):295–320.

34. Bonami P, Biegler LT, Conn AR, Cornuéjols G, Grossmann IE, Laird CD, Lee J, Lodi A, Margot F, Sawaya N, Wächter A. An algorithmic framework for convex mixed integer nonlinear programs. *Discret Optim*. 2008;5(2):186–204.
35. Quesada I, Grossmann IE. A global optimization algorithm for linear fractional and bilinear programs. *J Global Optim*. 1995;6(1):39–76.
36. Dowling AW, Dyreson A, Miller F, Zavala VM. Economic assessment and optimal operation of CSP systems with TES in California electricity markets. In: *AIP Conference Proceedings*, Vol. 1850. AIP Publishing, 2017:160006.
37. Kost C, Flath CM, Möst D. Concentrating solar power plant investment and operation decisions under different price and support mechanisms. *Energy Policy*. 2013;61:238–248.
38. Martín L, Martín M. Optimal year-round operation of a concentrated solar energy plant in the south of Europe. *Appl Thermal Eng*. 2013; 59(1–2):627–633.
39. Pousinho H, Contreras J, Pinson P, Mendes V. Robust optimisation for self-scheduling and bidding strategies of hybrid CSP fossil power plants. *Int J Electrical Power Energy Syst*. 2015;67:639–650.
40. Wittmann M, Eck M, Pitz-Paal R, Müller-Steinhagen H. Methodology for optimized operation strategies of solar thermal power plants with integrated heat storage. *Solar Energy*. 2011;85(4):653–659.
41. Poland J, Stadler KS. Stochastic optimal planning of solar thermal power. In: *IEEE Conference on Control Applications (CCA)*, 2014: 593–598.
42. Petrollese M, Cocco D, Cau G, Cogliani E. Comparison of three different approaches for the optimization of the CSP plant scheduling. *Solar Energy*. 2017;150:463–476.
43. Kim K, Zavala VM. Algorithmic innovations and software for the dual decomposition method applied to stochastic mixed-integer programs. *Technical Report, Argonne National Laboratory*, 2015.
44. Chiang N, Zavala V. An inertia-free filter line-search algorithm for large-scale nonlinear programming. *Comput Optim Appl*. 2016;64(2): 327–354.

Manuscript received Aug. 17, 2017, and revision received Dec. 19, 2017.